RESEARCH ARTICLE

Determination of oscillation frequencies and stellar properties of three Delta Scuti variable stars using Kepler data

J Adassuriya[1*], KPSC Jayaratne[2], PTLV Cooray[3] and MLC Attygalle[3]
[1] Astronomy Division, Arthur C Clarke Institute, Katubedda, Moratuwa.
[2] Department of Physics, Faculty of Sciences, University of Colombo,Colombo 03.
[3] Department of Physics, Faculty of Applied Sciences, University of Sri Jayewardenepura, Nugegoda.

Abstract: Asteroseismology is the science that deals with the oscillations in the stars with the goal of understanding the stellar structure. In this study, photometric data of Kepler mission have been used for the asteroseismic study of Delta Scuti type pulsating stars. The light curve analysis of three short cadences Kepler datasets of Delta Scuti stars has been presented. The pulsation frequencies were determined by applying a discrete Fourier transformation with the pre-whitening process. The full light curve of Kepler target KIC 9700322 revealed dominant radial fundamental frequency at 9.792 ± 0.002 d^{-1} and 1st overtone frequency at 12.569 ± 0.002 d^{-1} accompanied by a large number of frequency multiples. Non-radial frequencies of mode $l = 2$ quintuplet were detected with the frequency spacing of 0.134 d^{-1} and it provided a rotation period of the star as 6.19 days, which was detected as the peak of 0.159 d^{-1} in frequency spectra. Using the fundamental period, a value for relative density of the star was estimated as 0.10 ± 0.04 relative to the sun. Furthermore, the full dataset of KIC 11754974 was subjected to frequency analysis and the radial fundamental pulsation frequency and its 1st overtone were detected at 16.3451 ± 0.0002 d^{-1} and 21.3997 ± 0.0002 d^{-1}, respectively. $l = 2$ frequency quintuplet was detected with a frequency spacing of 0.22 d^{-1} and determined the rotation period and relative density of the star as 3.83 days and 0.29 ± 0.01, respectively. KIC 9845907 was identified as a purely radial pulsator. The fundamental pulsation frequency was recovered as 17.597 ± 0.002 d^{-1} with two other dominant modes of overtones at 22.850 ± 0.002 d^{-1} and 28.210 ± 0.002 d^{-1}. The relative density of the star was determined as 0.34 ± 0.06.

Keywords: Delta Scuti, oscillation modes, photometry, stellar pulsations.

INTRODUCTION

Astrophysics is the science that deals with understanding the physical and chemical phenomena related to celestial objects such as stars, galaxies and other celestial objects. Asteroseismology is an area in astrophysics devoted to the study of stellar oscillations, which probes the extreme status of temperature, density and pressure in stellar interiors (Guzik, 1997). Delta Scuti are a class of intrinsic variable stars, which consists of pure radial or multiple non-radial pulsation modes (Breger, 1976; Breger, 2020; Pakstiene *et al.*, 2018).

Stellar oscillations mainly depend on the resonant frequencies of standing waves of sound inside a star. The speed of sound depends on the temperature and chemical composition of the gas. By 'listening' to these sounds intrinsic stellar properties such as temperature, gravity, chemical composition etc, can be determined. Asteroseismology is equivalent to identifying musical notes by listening to the audio response. This field is developed with the advent of helioseismology, which studies the internal structure of the sun through the observed oscillations. Most importantly, the solar interior structure was determined by observing oscillation modes using photometry (Buldgen *et al.*, 2019).

The field of asteroseismology has been in rapid development because of the space telescopes, such as

*Corresponding author (adassuriya@gmail.com; https://orcid.org/0000-0002-6070-956x)

COROT and Kepler. Unlike ground-based observatories affected by telluric turbulence and weather, space-based observatories can receive high quality, photometrically stable and temporally reliable data. Asteroseismic investigations are not limited to only solar-like stars but it could also be applied to many different types of stars.

In this investigation, asteroseismic techniques were applied to δ Scuti type variable stars. δ Scuti stars (DSS) are located where the classical instability strip crosses the main sequence of the Hertzsprung-Russell (H-R) diagram. They are very short period pulsators; typically the pulsation period is less than one day (Breger, 2000). The radial pulsations are more general in DSS while non-radial oscillations are also present. In brief, non-radial pulsation modes can be described by three quantised numbers *n*, *l* and *m*, where *n* is the radial nodes between centre and surface, *l* is the number of nodes on the surface, and *m* represents the surface nodes which pass through the pulsation axis (Aerts *et al*., 2010). DSS have been discovered with short (periods of a few minutes) and long (periods of an hour or two) periods associated with pressure (p-modes) and gravity (g-modes) modes, respectively. Gravity mode pulsations are deep interior modes, which exhibit asymptotic period spacing for radial nodes with *l* << n (Reed *et al*., 2011).

DSS are at the stellar evolutionary stage of core or shell hydrogen burning. Therefore, DSS are in the transition phase of convective to radiative energy transport and assists in understanding the physics of the transition phase of stars (Aerts *et al*., 2010).

DSS were selected from the database of Kepler Asteroseismic Science Operations Center (KASOC). KASOC provides asteroseismological data from the Kepler mission to astronomers who are members of the Kepler Asteroseismic Science Consortium (KASC). Three Delta Scuti stars, KIC 9700322, KIC 11754974 and KIC 9845907 (KIC = Kepler Input Catalogue, Brown *et al*., 2011) observed by Kepler mission were selected for this analysis. KIC 9700322, KIC 11754974 and KIC 9845907 stars were mainly selected based on the presence of many frequencies in their power spectra as well as complex frequency combinations and spacing. The frequency spacing was explained as simple combinations of frequencies arising from non-linearity of the oscillation and hence provides information of physical properties of the stars. The observational details of these stars are listed in Table 1. These targets were selected based on higher coverage of observation and the availability of oscillation frequencies in their light curves.

Table 1: Summary of observational parameters of selected δ Scuti stars. K_p is the Kepler magnitude

Star	R.A.	Dec.	K_p	Kepler quarters	Data points
KIC 9700322	19h 07m 50.7s	46° 29 12	12.685	Q11.1	45184
				Q11.2	43543
				Q11.3	46311
				Q12.1	34037
				Q12.2	39984
				Q12.3	32946
KIC 11754974	19h 08m 15.9s	49° 57 15	12.678	Q6.1	39630
				Q6.2	45255
				Q6.3	43996
				Q7.1	44036
KIC 9845907	19h 49m 30.4s	46° 40 02	11.640	Q8.1	45184
				Q8.2	38648
				Q8.3	29390
				Q9.1	53282
				Q9.2	41711
				Q9.3	45616

Asteroseismology of a star highly depends on the precise determination of oscillation frequencies among artifacts generated by different sources such as frequency aliasing in ground-based data and periodic changes of the space observatories such as reorientations, safe-modes, etc (Garcia *et al*., 2011). Signal-to-Noise (S/N) ratio of the frequency spectrum is another major issue of demarcation of stellar frequencies.

METHODOLOGY

Kelper light curves

The Kepler space telescope was launched in 2009 to search Earth-like planets. The period of Earth trailing orbit of the satellite is 372.5 days. The observations were focused on 115 square degrees field of view in the constellation of Cygnus and Lira (Garcia *et al*., 2011). The stars were observed in Kepler magnitude (K_p) in the wavelength range of 430 – 890 nm. The K_p is defined as AB magnitudes (Oke, 1974, Smith *et al*., 2002) derived from each target's calibrated g, r, i magnitudes. Details of the K_p is available in Brown *et al*. (2011). Kepler observations are made in two different operating modes: Long-Cadence (LC) targets are sampled every 29.5 min (Nyquist frequency of 283.45 µHz) and Short-Cadence (SC) every 58.5 s of exposure (Nyquist frequency of ~8.5 mHz) (Garcia *et al*., 2011). SC light curves of DSS were used allowing the high resolution of power spectra which can resolve frequencies up to 100 cycles per day (1.16 µHz). We used the corrected flux by the KASOC database and performed further corrections of eliminating photometric jumps and outliers, and linear trends for every quarter in SC data. The full light curve of quarter 11 and 12 of KIC9700322 is shown in Figure 1. The time stamp of the light curves is in Barycentric Julian Date (BJD). From quarter to quarter of the Kepler's observation, the mean flux levels of stars were considerably changed as shown in the top panel of Figure 1. To reorient spacecraft solar arrays, the Kepler satellite performed quarterly rolls (every 93 days) resulting in quarterly discontinuities in the mean flux levels of observed stars; specifically, the roll displaces a star between the 42 charge couple device (CCD) modules, which comprises the field-of-view with the modules having different characteristics (*http://kplerscience.arc.nasa.gov/the-kepler-space-telescope. html*). Furthermore, changes in the average flux also occur within the quarter. In order to remove inter- and intra-quarter offsets, the medians of the two quarters were obtained by fitting linear polynomials and then quarter 12 was shifted by the difference of two medians (Figure 1).

The normalised two quarters were again approximated by third order polynomial for the conversion of parts per million (ppm) as shown in the bottom panel of Figure 1. Using the polynomial, the Kepler flux [$F_{Kp}(t)$] was reduced to a fractional quantity (ppm) with respect to the broad, underlying baseline characterised by a polynomial f(t), using the equation 1.

$$F_{ppm}(t) = 10^6 * \left(\frac{F_{kp}(t)}{f(t)} - 1 \right) \qquad ...(1)$$

Polynomials were tested with order in the range 2–10 that best represented the baseline of the shifted quarters. It was found that the third or fourth order polynomials sufficiently fit the overall baseline and provide a better fit than a linear baseline. A part of a light curve after the conversion to ppm is shown in Figure 2. This conversion process of flux improves the S/N ratio of the power spectrum and hence possible to determine the weak frequency signals.

Frequency analysis

The amplitude spectrum of each star as a function of time, t, was expressed using a Fourier representation based on the harmonic term sum in equation 2.

$$m = m_0 + \sum_{i=1}^{N} A_i sin[2\pi(f_i t + \Phi_i)] \qquad ...(2)$$

where m_0 is the zero-point and A_i, f_i and ϕ_i are the amplitude, frequency and phase of the ith term, respectively.

Period04 (Lenz & Breger, 2005) software package was used to compute the discrete Fourier transformation (DFT) power spectrum of the light curves as shown in Figures 3, 4 and 5, respectively for KIC 9700322, KIC 9845907 and KIC 11754974. Period04 detects dominant frequencies in the amplitude spectra and calculates the amplitude and the phase of the detected frequencies. The frequencies were searched with the step size of 0.0098 µHz and pre-whitening process applied, which subtracts the detected frequencies from the light curve before searching the next frequency. The 'a', 'b', 'c' and 'd' subplots in Figures 3, 4 and 5 consecutively represent the frequencies determined by the pre-whitening process after removing the previous strongest peak. The pre-whitening process recovers frequencies from the residual light curve. The process of pre-whitening is very useful to extract the frequencies of the star from the amplitude spectrum, and particularly the unwanted frequency peaks can be avoided, which otherwise arise due to aliases.
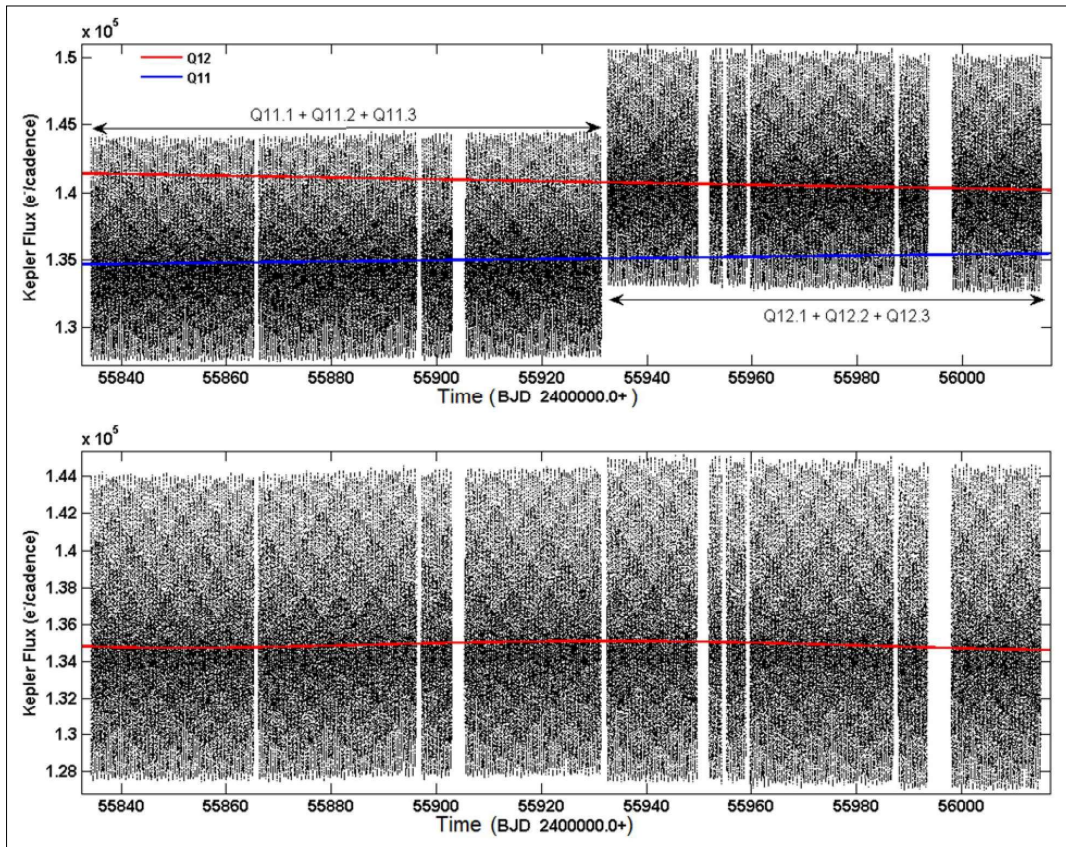
Figure 1: Upper: Kepler flux of KIC9700322 for the quarters of 11 and 12. The blue and red lines indicate the linear best fits of the quarter 11 and 12, respectively. Lower: The two quarters shifted to the median of each dataset. The red line indicates the best fit polynomial used for the conversion of ppm.
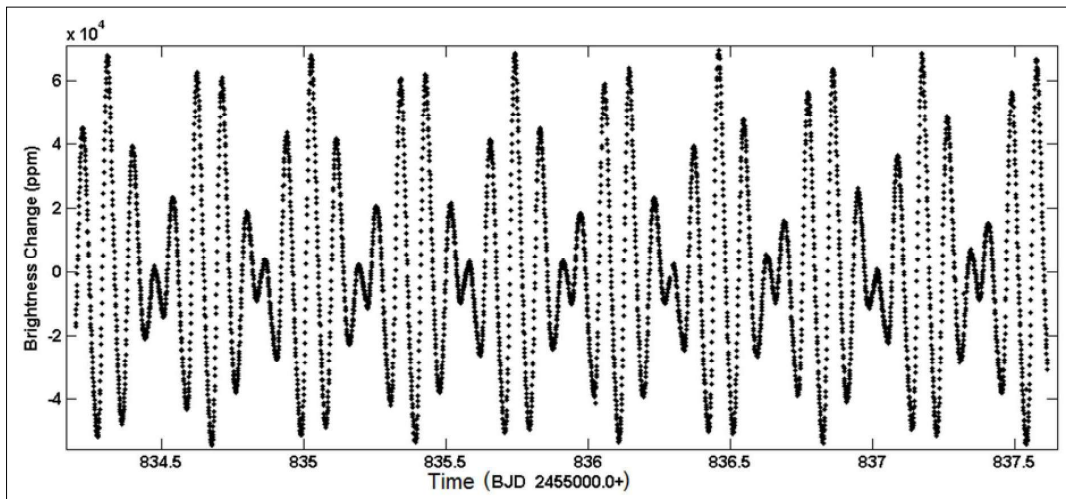

Figure 2: Part of the light curve of KIC 9700322 after converting to ppm

The amplitude detection threshold of the frequency spectrum was calculated using the region of free form pulsations. When the S/N ratio is less than 4 magnitudes (Baran *et al*., 2012), the signal is no longer considered statistically significant. This criterion was followed to terminate the frequency detection process so that the successive pre-whitening stops when the peak of the highest-amplitude in the periodogram has a value, which is considered too small to be significant.

Frequency combinations and the equidistant frequency patterns

Most of the overtones and linear combinations of the frequencies in the power spectrum can be expressed in a very simple way through a general equation $f = mf_1 \pm nf_2$ where m and n are small integers and f_1 and f_2 are two frequencies with the highest amplitudes in the power spectrum. These frequencies are called dominant

Table 2: Frequencies of KIC 9700322 given in cycles per day and µHz. Amplitudes are in parts per million (ppm). The major modes are also identified.

Frequency (cycles/day) ±0.002	Frequency (µHz)	Amplitude (ppm)	Identification	Comment
Main frequencies				
9.792	113.34	1227651.58	f1	Fundamental
12.569	145.48	1319764.29	f2	1st Overtone
0.159	1.85	4583.00	f3	Rotation
0.0121	0.14	46826.81	f4	
11.316	131.02	6348.07	f5	Quintuplet
11.455	132.58	5775.80	f6	Quintuplet
11.589	134.14	22978.14	f7	Quintuplet
11.719	135.64	10042.14	f8	Quintuplet
11.858	137.25	5230.76	f9	Quintuplet
Frequency combinations				
0.026	0.31	11464.82	2f4	
2.775	32.13	122446.58	f2-f1	
5.550	64.24	5982.86	2f2-2f1	
7.016	81.21	28803.27	2f1-f2	
9.781	113.21	13594.57	f1+f2-f3	
9.792	113.48	8693.03	f1+f2-f3+2f4	
12.545	145.19	96857.34	f2-2f4	
12.569	145.35	67945.97	f2-f4	
12.582	145.63	14856.26	f2+f4	
15.345	177.61	23618.59	2f2-f1	
19.585	226.68	102097.16	2f1	
22.361	258.81	225738.91	f1+f2	
25.137	290.94	126096.23	2f2	
27.914	323.08	9578.32	3f2-f1	
29.377	340.01	5754.46	3f1	
32.153	372.15	23401.58	2f1+f2	
34.929	404.28	24567.54	f1+2f2	
37.705	436.41	14988.67	3f2	
44.723	517.63	6819.39	2f1+2f2	
62.541	723.86	5842.42	5f2	

frequencies. Additional patterns are also identified using the rotational frequency of the star. Most of the detected frequencies can be identified as part of regular patterns. By using this methodology, the dominant frequencies

in the data were identified and are given in Tables 2, 3 and 4, respectively for KIC 9700322, KIC 11754974 and KIC 9845907.

Table 3:   Frequencies of KIC 11754974 given in cycles per day and µHz. Amplitudes are in parts per million (ppm). The major modes are also identified.

Frequency (cycles/day) ± 0.0002	Frequency (µHz)	Amplitude (ppm)	Identification	Comment
Main frequencies				
19.7839	228.98	85.08	f6	Quintuplet
20.0194	231.71	102.61	f7	Quintuplet
20.2437	234.30	125.27	f8	Quintuplet
20.4562	236.76	68.22	f9	Quintuplet
20.6560	239.07	51.71	f10	Quintuplet
Frequency combinations				
0.4921	5.70	102.97	f2-f3	
1.2605	14.59	86.04	f5-f2	
4.5624	52.81	559.64	f3-f1	
4.5990	53.23	271.40	f4-f1	
5.0546	58.50	532.20	f2-f1	
6.3159	73.10	90.36	f5-f1	
11.2905	130.68	251.95	2f1-f2	
11.7461	135.95	69.57	2f1-f4	
11.7826	136.37	224.09	2f1-f3	
15.8530	183.48	54.36	f1-f3-f2	
26.4542	306.18	60.32	2f2-f1	
27.6356	319.86	56.36	3f1-f2	
28.1277	325.55	53.22	3f1 − f3	
32.6902	378.36	1505.81	2f1	
37.2518	431.16	467.73	f1 + f3	
37.2900	431.60	391.97	f1 + f4	
37.7447	436.86	695.09	f1 + f2	
39.0061	451.46	63.36	f1 + f5	
41.8151	483.97	58.96	2f3	
41.8533	484.41	92.22	f4 + f3	
42.3072	489.67	137.90	f2 + f3	
42.7993	495.36	102.06	2f2	
49.0353	567.54	329.11	3f1	
53.5969	620.34	149.79	2f1 + f3	
53.6351	620.78	96.23	2f1 + f4	
54.0898	626.04	158.53	2f1 + f2	
59.1444	684.54	83.70	2f2 + f1	
65.3804	756.72	74.84	4f1	

Table 4: Frequencies of KIC 9845907 given in cycles per day and µHz. Amplitudes are in parts per million (ppm). The major modes are also identified.

Frequency (cycles/day) ± 0.002	Frequency (µHz)	Amplitude (ppm)	Identification	Comment
Main frequencies				
17.597	203.67	10496.36	f1	Fundamental
22.850	264.51	2636.76	f2	1st Overtone
28.210	326.56	530.07	f3	2nd Overtone
0.065	0.75	450.92	f4	
13.831	160.08	195.37	f5	
27.010	312.62	685.87	f6	
Frequency combinations				
1.693	19.60	151.43	f2-f1	
13.898	160.85	136.75	f3+f4	
26.880	311.11	192.45	f6-2f4	
26.945	311.86	156.26	f6-f4	
28.956	335.13	226.29	f6 + 3f4	
29.736	344.17	448.16	2f5 -f6 + f4	
29.797	344.88	163.88	2f5 -f6 + 2f4	
31.363	363.00	1181.84	f1+f5 -f4	
31.428	363.75	2209.07	f1 + f5	
31.493	364.51	1993.26	f1 + f5 + f4	
35.195	407.35	572.34	2f1	
49.025	567.42	176.29	f1 + f2	
49.090	568.17	125.97	f1 + f2 + f4	
59.471	688.32	393.34	4f5 -2f6 +2f4	
61.164	707.92	324.04	2f1 + f2 - 2f4	
62.856	727.50	315.41	2f1 + 2f5	
77.070	892.00	163.59		

The next step is the identification of radial modes and non-radial modes. In radial pulsating stars the period ratios of the modes are good approximations of mode identification. For DSS, the theoretically expected period ratio of fundamental radial (P_1) and first radial overtone (P_2) pulsation (P_2/P_1) is 0.756 – 0.789 (Stellingwerf, 1979). The ratio of second overtone period (P_3) to the fundamental (P_3/P_1) is 0.611 – 0.632 (Stellingwerf, 1979). However, the period ratios also depend on metallicity, stellar rotation period, stellar mass and density (Mirouh *et al*., 2019). The higher metallicity and higher rotational velocity increase the period ratios around 10^{-3} (Breger, 2000; Paparo *et al*., 2017). By using the period ratios, the radial modes of fundamental, first harmonic and second

harmonic were identified, which fall well within the above mentioned ranges and shown in Tables 2, 3 and 4. The frequency multiplets can be used to identify the degree, l, as $2l + 1$ produce azimuthal modes m, so that $l = 1$ produces triplets with -1, 0 and +1, $l = 2$ produces quintuplets of -2, -1, 0, +1, and +2. These frequency separations depend on the value of degree l. Therefore, evenly spaced peaks in frequency may help to identify l values (Paparó *et al*., 2013). In order to recover the frequency separations all detected frequencies were arranged in ascending order for the three targets. The identified equidistant frequency patterns for KIC 9700322 and KIC 11754974 are given in Tables 2 and 3, respectively.

Determination of stellar properties

The stellar rotation period (P_{rot}) of a star can be written as,

$$P_{rot} = \frac{1 - C_{n,l}}{v_{n,l,m} - v_{n,l,0}} \qquad ...(3)$$

Where $v_{n,l,m}$ is the observed frequency and $v_{n,l,0}$ is the unperturbed central frequency of the multiplet for $m = 0$, which is unaffected by the rotation. $C_{n,l}$ expresses the Ledoux constant (Ledoux, 1951) which determines the usual equidistance splitting valid in the limit of slow rotation (Goupil *et al*., 2000) and $C_{n,l} \approx \dfrac{1}{l(l+1)}$ for g-modes and negligibly small for p-modes. By using this equation the stellar rotation period was determined.

By knowing the splitting, *m*, and the Ledoux constant, it is possible to calculate the stellar rotation period. The frequency splitting $\Delta v_{n,l,m}$ is the difference of $v_{n,l,m}$ and $v_{n,l,0}$. The frequency splitting observed from spectra for KIC 9700322 is 0.134 d^{-1} for $l = 2$ quintuplet and for KIC 11754974 it is 0.218 d^{-1} for the same degree of $l = 2$. The Ledoux constant $C_{n,l}$ for $l = 2$ quintuplet is 0.164 (Kurtz, 2014). By substituting these values in the above equation, the value of rotation period (P_{rot}) was calculated.

Furthermore, the pulsation constant Q is defined as;

$$Q = P_1 \sqrt{\frac{\rho}{\rho_\odot}} \qquad ...(4)$$

P_1 is the fundamental pulsation period in days, and ρ is the mean stellar density, which is normalised to the solar value . Substitution of Q for the radial fundamental mode, 0.033 d (Breger & Bregman, 1975; Balona *et al*., 2012) with the determined fundamental periods in equation 4 provides the relative mean densities of three DSS. The error estimation of the computation was taken from the propagation error of the frequency. The frequency error was taken as the standard deviation of hundred iterations of Monte Carlo simulation in Period04.
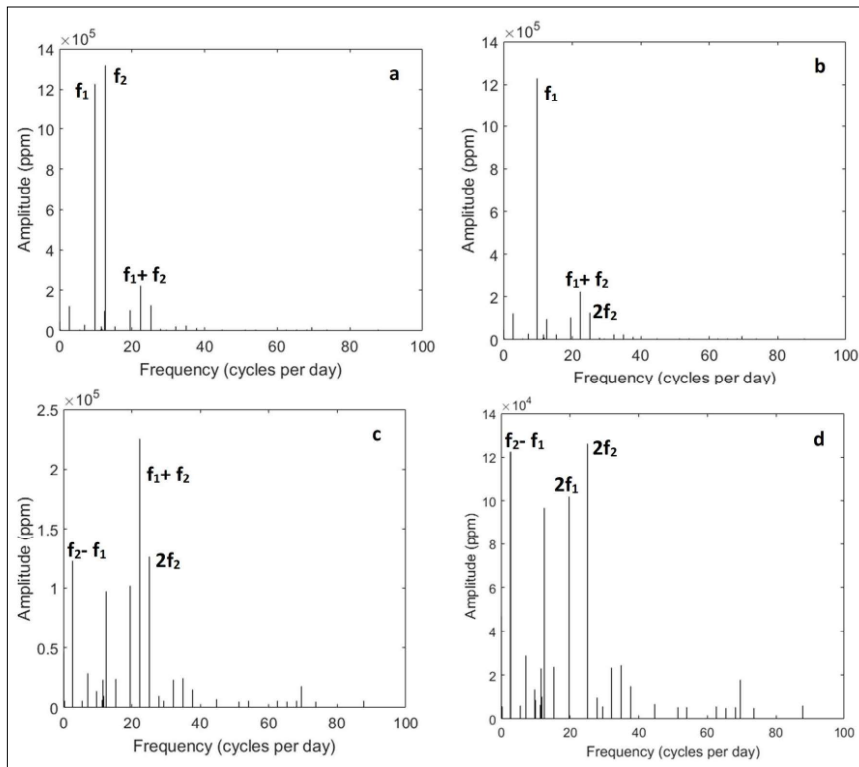

Figure 3:   Amplitude spectra of KIC 9700322. The oscillation frequencies are seen as sharp peaks. The panels a, b, c and d show the remaining frequencies after pre-whitening the dominant frequency.

Figure 4: Amplitude spectra of KIC 9845907. The oscillation frequencies are seen as sharp peaks. The panels a, b, c and d show the remaining frequencies after pre-whitening the dominant frequency.

Figure 5: Amplitude spectra of KIC 11754974. The oscillation frequencies are seen as sharp peaks. The panels a, b, c and d show the remaining frequencies after pre-whitening the dominant frequency.
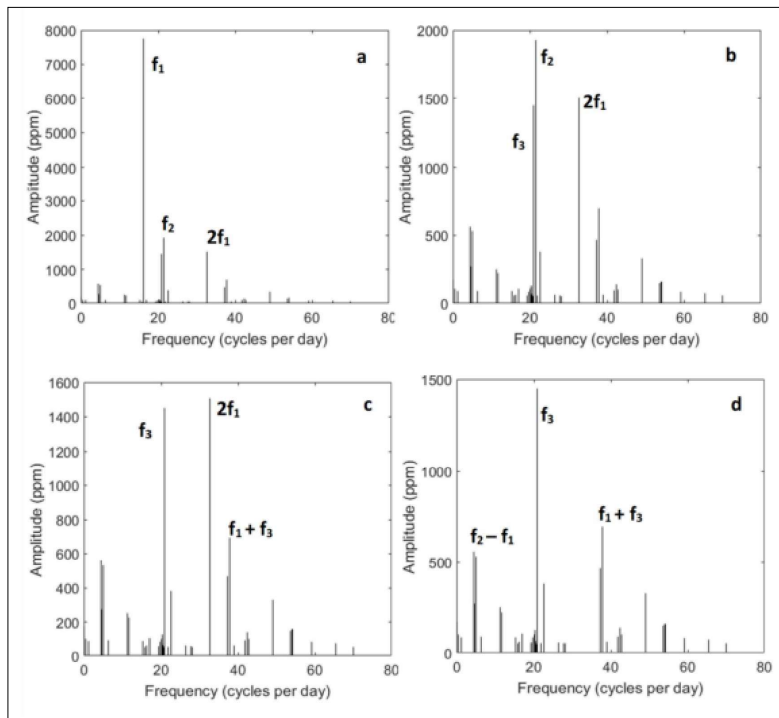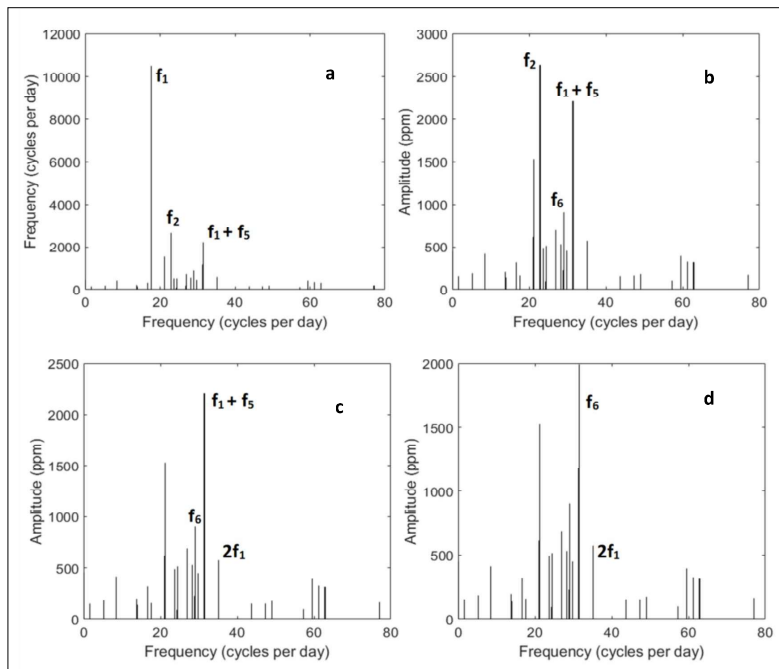
RESULTS AND DISCUSSION

KIC 9700322

The full dataset of KIC 9700322 from quarter 11.1 (Q11.1) through quarter 12.3 (Q12.3) was obtained from the KASOC. For a total of 242005 data points spanning a total time of 180 days after normalisation, the pulsation frequencies were determined by applying discrete Fourier transformation (DFT) signal processing using Period04 software. The oscillation frequencies were searched in the range of 0 µHz to 1157.41 µHz in 0.0093 µHz step size. The pulsation frequencies of KIC 9700322 are listed in Table 2. This target was also observed and analysed for frequencies by Breger, *et al.* (2011). Both analyses derived the same set of prominent frequencies with $l = 2$ quintuplet. In addition, this analysis confirmed the fundamental frequency as 9.792 d^{-1} and first overtone as 12.569 d^{-1} using the period ratio method. Furthermore, the relative density of KIC 9700322 $(\frac{\rho}{\rho_\odot})$ was determined as 0.10 ± 0.04. The period ratios of P_2/P_1 of this star is 0.779 which is quite high compared to the 0.687 (Böhm-Vitense, 1992) for more realistic polytrope of $n = 3$, where n is the polytrope index. For higher n, there should be higher mass concentration towards the centre of a star, which represents a real star. Therefore, the higher P_2/P_1 ratio of KIC 9700322 implies higher central density concentration. In 2014, Suarez *et al.* (2014), showed the relationship of large frequency separation and mean density of DSS. According to this prediction the relative mean density of 0.10 ± 0.04 is compatible with the fundamental frequency of 9.792 d^{-1} (113 µHz). In general, the upper limit of mass of DSS is 2.5 $M_\odot$ (Aerts *et al.*, 2010). Therefore, the upper limit of the radius of KIC 9700322 can be estimated as 2.9 ± 0.3 $R_\odot$.

KIC 11754974

The full dataset of KIC 11754974 from quarter 6.1 (Q6.1) through quarter 7.1 (Q7.1) was obtained from the KASOC. For 172917 data points, spanning a total time of 120 days after normalisation, the pulsation frequencies were determined by the same method as in KIC 9700322. The oscillation frequencies were searched in the range of 0 µHz to 1157.41 µHz in the step size of 0.0098 µHz. The pulsation frequencies of KIC 11754974 are listed in Table 3. The determined relative density using the period-density relationship of KIC 11754974 is 0.29 ± 0.01. The upper limit of the radius is 1.86 ± 0.02 for the standard upper mass of 2.5 of DSS stars.

KIC 9845907

The full dataset of KIC 9845907 from quarter 8.1 (Q8.1) through quarter 9.3 (Q9.3) was obtained from the KASOC. This star was observed in 171 days resulting 253831 flux values. The frequency analysis was done using Period04 in the range of 0 µHz to 1157.41 µHz in the step size of 0.0098 µHz. The pulsation frequencies of the KIC 9845907 are listed in Table 4. A mean relative density $(\frac{\rho}{\rho_\odot})$ of 0.34 ± 0.06 revealed that this star has a maximum radius of 1.94 ± 0.09 $R_\odot$ for the upper ceiling of mass 2.5 $M_\odot$.

The dominant radial modes of KIC 9700322, KIC 11754974 and KIC 9845907

The frequency ratio of fundamental (f_1) and 1st harmonic (f_2) were calculated for all three stars. The ratios, f_1/f_2, for KIC 9700322, KIC 11754974 and KIC 9845907 are 0.779, 0.763 and 0.779, respectively. These values are close to the expected frequency ratio of fundamental and first overtone radial pulsation of DSS (Stellingwerf, 1979). Furthermore, the frequency ratio f_2/f_3, 1st overtone $(f_2 = 22.854 \text{ day}^{-1})$ and 2nd overtone $(f_3 = 28.214 \text{ day}^{-1})$ of KIC 9845907 is 0.81, which is close to the expected frequency ratio of 1st overtone and 2nd overtone for radial pulsation of DSS.

In mode identification, the simplest modes are the radial modes, which is represented by $l = 0$ and integer values of n for fundamental and its overtones. The frequency of fundamental radial mode $(n = 1)$ is known as f_1. In this mode, the star swells and contracts, heats and cools in spherical symmetry with the core as a node and the surface as a moving anti-node.

The frequency of the first overtone radial mode (f_2) which corresponds to $n = 2$, has one radial node that is a concentric shell within the star. As we are thinking in terms of the radial displacement, that shell is a non-moving node; the motions above and below the node move in anti-phase.

The ratio of the first overtone to the fundamental in DSS is a direct consequence of the sound speed gradient in them, hence of the temperature and (in some places) of chemical composition gradients. Thus, just by observing two pulsation frequencies we have had our first look into the interiors of KIC 9700322, KIC 11754974 and KIC 9845907.

The combination frequencies and the quintuplet

We can clearly identify that the detected frequencies of KIC 9700322 (Breger *et al*., 2010), KIC 11754974 and KIC 9845907 show simple linear combinations of f_1 and f_2 and the rotational frequency. These combinations help in identifying the radial modes. For non-radial modes, combination frequencies are not allowed.

In the frequency spectrum of KIC 9700322 and KIC 11754974 we can clearly identify the equidistant frequency pattern of peaks with a number of components, which depends on the value of *l*. These five peaks (quintuplet) for $l = 2$ is given by the equation $m = 2l + 1$. Therefore, in $l = 2$ mode, there are five peaks possible as -2, -1, 0, +1 and +2 where the central peak is denoted as $m = 0$.

In KIC 9700322, quintuplet was found (f_5, f_6, f_7, f_8 and f_9 in Table 2) around the two dominant modes and the average spacing between the frequencies in the quintuplet was 0.134 day^{-1}. In KIC 11754974, quintuplet was found (f_6, f_7, f_8, f_9 and f_{10} in Table 3) around the two dominant modes and the average spacing between the frequencies in quintuplet was 0.2180 day^{-1}. This value is identified as the frequency splitting ($\Delta v_{n,l,m}$) in equation 3. The rotation period (P_{rot}) and rotation frequencies can be calculated by using this frequency splitting.

The stellar rotation period (P_{rot})

For the star KIC 9700322, the frequency splitting of $\Delta v_{n,l,m} = 0.134$ d^{-1} was substituted in equation 3 and the value of rotation period (P_{rot}) was estimated. The rotation period was 6.19 days, which means the rotational frequency is 0.1614 day^{-1}. We observed a frequency value $f_3 = 0.159$ d^{-1} in Table 2 which is closer to the value calculated above. Therefore, it can be determined that f_3 is the rotational frequency of KIC 9700322. This result also confirmed that the rotational frequency is much smaller than the pulsation frequency of DDS. Similarly for KIC 11754974, the value $\Delta v_{n,l,m}$ was 0.218 d^{-1} and the rotation period (P_{rot}) is 3.8348 days. The rotational frequency was 0.260 d^{-1}. However, this frequency could not be recovered from the power spectra of KIC 11754974.

CONCLUSIONS

The frequency analysis of three high-amplitude δ Scuti stars observed with the Kepler spacecraft named, KIC 9700322, KIC 11754974 and KIC 9845907 was presented. More than 180 days of continuous observations of short cadence Kepler data was used to detect 41 independent frequencies in KIC 9700322, 50 frequencies in KIC 11754974 and 40 frequencies in KIC 9845907. KIC 9700322, KIC 11754974 and KIC 9845907 stars were mainly selected based on the presence of many frequencies in their power spectra as well as complex frequency combinations and spacing. The frequency spacing was explained as simple combinations of frequencies arising from non-linearity of the oscillation. Combination frequencies, the quintuplets (*l*=2 mode) and the estimations of relative densities and radii for all three stars were presented. In addition, the rotation periods were determined as 6.19 days and 3.83 days for KIC 9700322 and KIC 11754974, respectively. The values of relative densities $\frac{\rho}{\rho_{\odot}}$ were determined as 0.10 ± 0.04, 0.29 ± 0.01 and 0.34 ± 0.06 for KIC 9700322, KIC 11754974 and KIC 9845907, respectively. KIC 9700322 and KIC 11754974 both contain radial and non-radial pulsation while KIC 9845907 is only a radial pulsator.

REFERENCES

Aerts C., Christensen-Dalsgaard J. & Kurtz D.W. (2010). *Asteroseismology,* pp. 49–54. Springer Science and Business Media, New York, USA.
DOI: https://doi.org/10.1007/978-1-4020-5803-5

Balona L.A. *et al*. (23 authors) (2012). Kepler observations of the high amplitude delta suity star V2367 Cyg. *Monthly Notices of the Royal Astronomical Society* **419**(4): 3028–3038.
DOI: https://doi.org/10.1111/j.1365-2966.2011.19939.x

Baran A.S. *et al*. (11 authors) (2012). A pulsation zoo in the hot subdwarf B star KIC 10139564 observed by Kepler. *Monthly Notices of the Royal Astronomical Society* **424**(4): 2686–2700.
DOI: https://doi.org/10.1111/j.1365-2966.2012.21355.x

Böhm-Vitense E. (1992). *Introduction to Stellar Astrophysics*, volume 3, pp. 222–227. Cambridge University Press, UK.
DOI: https://doi.org/10.1017/CBO9780511623028

Brown T.M., Latham D.W., Everett M.E. & Esquerdo G.A. (2011). Kepler input catalog: photometric calibration and stellar classification. *The Astronomical Journal* **142**(4): 112.
DOI: https://doi.org/10.1088/0004-6256/142/4/112

Breger M. (2000). Delta Scuti stars (Review). *Astronomical Society of the Pacific Conference Series* 210: 3

Breger M. *et al.* (11 authors) (2011). Regularities in frequency spacings of δ Scuti stars: the Kepler star KIC 9700322. *Monthly Notices of the Royal Astronomical Society* **414**(2): 1721–1731.
DIO: https://doi.org/10.1111/j.1365-2966.2011.18508.x

Breger M. (1979). Delta Scuti and related stars. *Publications of the Astronomical Society of the Pacific* **91**(539): 5.
DOI: https://doi.org/10.1086/130433

Breger M. & Bregman J.N. (1975). Period-luminosity-color relations and pulsation modes of pulsating variable stars. *The Astrophysical Journal* **200**: 343–353.
DOI: https://doi.org/10.1086/153794

Breger M. (2000). Delta Scuti stars (Review). *Astronomical Society of the Pacific Conference Series* **210**: 3

Buldgen G., Salmon S. & Noels A. (2019). Progress in global helioseismology: a new light on the solar modelling problem and its implications for solar-like stars. *Frontiers in Astronomy and Space Sciences* **6**: 42.
DOI: https://doi.org/10.3389/fspas.2019.00042

García R.A. *et al*. (11 authors) (2011). Preparation of Kepler light curves for asteroseismic analyses. *Monthly Notices of the Royal Astronomical Society: Letters* **414**(1): L6–L10.
DOI: https://doi.org/10.1111/j.1745-3933.2011.01042.x

Goupil M.J., Dziembowski W.A., Pamyatnykh A.A. & Talon S. (2000). Rotational splitting of delta Scuti stars. In: *Delta Scuti and Related Stars: Reference Handbook and Proceedings of the 6th Vienna Workshop in Astrophysics*, volume 210 (eds. M. Breger & M.H. Montgomery), Vienna, Austria, 4–7 August 1999, Astronomical Society of the Pacific, p. 267.

Guzik J.A. (1998). Delta Scuti stars: theory. In: *New Eyes to See Inside the Sun and Stars* (eds. F. Deubner, J. Christensen-Dalsgaard & D. Kurtz), International Astronomical Union Symposium no. 185. Kyoto, Japan, 18–22 August 1997, p. 331.
DOI: https://doi.org/10.1007/978-94-011-4982-2_74

Kurtz D.W. (2014). Asteroseismic measurement of surface-to-core rotation in a main-sequence A star, KIC 11145123. *Monthly Notices of the Royal Astronomical Society* **444**: 102–116.
DOI: https://doi.org/10.1093/mnras/stu1329

Ledoux P. (1951). The nonradial oscillations of gaseous stars and the problem of beta Canis Majoris. *The Astrophysical Journal* **114**: 373.
DOI: https://doi.org/10.1086/145477

Lenz P. & Breger M. (2005). Period04 user guide. *Communications in Asteroseismology* **146**: 53–136.
DOI: https://doi.org/10.1553/cia146s53

Mirouh G. M., Angelou G.C., Reese D.R. & Costa G. (2019). Mode classification in fast-rotating stars using a convolutional neural network: model-based regular patterns in δ Scuti stars. *Monthly Notices of the Royal Astronomical Society: Letters* **483**(1): L28–L32.
DOI: https://doi.org/10.1093/mnrasl/sly212

Oke J.B. (1974). Absolute spectral energy distributions for white dwarfs. *The Astrophysical Journal Supplement Series* **27**: 21.
DOI: https://doi.org/10.1086/190287

Pakštienė E., Janulis R., Tautvaišienė G., Drazdauskas A., Klebonas L., Mikolaitis Š., Minkevičiūtė R. & Bagdonas V. (2018). Variability analysis of δ Scuti candidate stars. *Publications of the Astronomical Society of the Pacific* **130**(990): 084201.
DOI: https://doi.org/10.1088/1538-3873/aac5cf

Paparó M. *et al*. (13 authors) (2013). CoRoT 102749568: mode identification in a δ Scuti star based on regular spacings. *Astronomy and Astrophysics* **557**: A27.
DOI: https://doi.org/10.1051/0004-6361/201321792

Paparó M. *et al*. (11 authors) (2017). The delta Scuti star 38 Eri from the ground and from space. *Monthly Notices of the Royal Astronomical Society* **477**(4): 4362–4379.
DOI: https://doi.org/10.1093/mnras/sty885

Reed M.D. *et al*. (11 authors) (2011). First Kepler results on compact pulsators-VIII. Mode identifications via period spacings in g-mode pulsating sub dwarf B stars. *Monthly Notices of the Royal Astronomical Society* **414**: 2885–2892.
DOI: https://doi.org/10.1111/j.1365-2966.2011.18532.x

Smith J.A. *et al*. (11 authors) (2002). The ugriz standard-star system. *The Astronomical Journal* **123**(4): 2121.
DOI: https://doi.org/10.1086/339311

Stellingwerf R.F. (1979). Pulsation in the lower Cepheid strip. I - linear survey. *The Astrophysical Journal* **227**: 935–942.
DOI: https://doi.org/10.1086/156802

Suárez J.C., Hernández A. G., Moya A., Rodrigo C., Solano E., Garrido R. & Rodón J.R. (2014). Measuring mean densities of δ Scuti stars with asteroseismology-theoretical properties of large separations using TOUCAN. *Astronomy and Astrophysics* **563**: A7.
DOI: https://doi.org/10.1051/0004-6361/201322270